Unexpected Fluorescent Behavior of Maleimide Based Zwitterionic Molecule: Aggregation Induced Emission

Ishita Mukherjee*

[a]*Department of Chemistry, The University of Burdwan, Burdwan-713104, West Bengal, India*

* Corresponding Author: E-mail: ishitamukherjee08@gmail.com

Ishita Mukherjee, Ph.D. IISER-Kolkata
Gold Medalist
Research Associate
Chemistry Department, Carbohydrate Lab, The University of Burdwan,
Burdwan 713104, WB, India
Phone: +91-9804980332
E-mail: ishitamukherjee08@gmail.com

To contribute through dedication, hard work and sincerity towards the overall growth of the organization; wherein she gets the opportunity of explore her academic, technical and scientific knowledge and prove her credentials as a reputed professional. She is currently working as a postdoctoral research associate in the University of Burdwan, West Bengal, India in the field of "**synthetic carbohydrate polymeric gel and their biomedical applications**" after completing her doctorate degree from Indian Institute of Science Education and Research (IISER) Kolkata, West Bengal, India on "**polymer synthesis from renewable sources and their antibacterial applications**". She is developing her research expertise on synthesis, characterization and biological applications of some injectable *in situ* forming polysaccharide-based gel; synthesis of polymers from renewable resources and amino acid-based monomers *via* controlled radical polymerization techniques; multistep organic synthesis; development of antibacterial system; protein immobilization through natural or synthetic polymer support. She has achieved University Gold Medal for her first class first position in Masters. She has been awarded as CAS Registry Innovator for innovation of novel substances as identified by Chemical Abstract Service (A Division of the American Chemical Society), Research Excellence Award by Institute of Scholars (InSc), Govt. of India, Best Poster Award in scientific international conference to celebrate 70th anniversary of India-Russia Diplomatic Relations. She is a professional reviewer and lifetime member of the InSc; regular member of American Chemical Society (ACS) and Royal Society of Chemistry (RSC). Currently she has joined as a peer reviewer in STAR Protocol, Elsevier after achieving a Certificate of Excellence in Certified Peer Review Course by Research Academy, Elsevier, UK and graduated from ACS Reviewer Lab.

Unexpected Fluorescent Behavior of Maleimide Based Zwitterionic Molecule: Aggregation Induced Emission

ABSTRACT: A novel traditional fluorophore free bright blue light emitting small organic molecule with aqueous solubility consisting *N*-substituted maleimide with zwitterionic side chain was explored. The combined experimental and theoretical studies revealed that the fluorescence originated due to the aggregation of *N*-substituted maleimide molecules named *N*-(ethyl sulfobetaine) maleimide (**M**) in solution. It was also observed that the aggregation induced emission (AIE) was originated after certain threshold concentration which was confirmed by both the experiment and the first principal calculations. The aggregation of the **M** molecule in solution happens predominantly due to nonbonded electrostatic interaction. This finding may add a new dimension to broad sensing application with a feasible molecular strategy.

Keywords: fluorophore, zwitterionic, aggregation induced emission (AIE)

1. INTRODUCTION

The breakthroughs in the understanding and applications of the light-emitting procedures have unwrapped new opportunities to scientific advancement and social development as light is the most fundamental constituent of life in universe. Light is emitted from fluorescent bioprobes in presence or absence of fluorophoric functionality, which typically contain several combined aromatic groups, or planar or cyclic molecules with several π-bonds resulting extended conjugation,[1] producing expected and unexpected fluorescence respectively. The development of sensitive and selective fluorescent bioprobes is of great importance in biological science and technology,[2] such as bioimaging[3] and monitoring biological species,[4,5] bacterial detection,[6] drug delivery,[7] labelling of protein or amino acids, DNA probing[8] along with several practical sensing applications.[9] Various inorganic fluorescent nanoparticles such as semiconductor quantum dots,[10] lanthanide ion doped nanomaterials,[11] fluorescent carbon dots,[12] metallic nanoclusters and photoluminescent silicon nanoparticles[13] are most extensively used in biomedical purposes over the past few decades. Several disadvantages like difficult synthetic procedure, blinking effect, non-

biodegradability, potential toxicity due to their accumulation in the reticuloendothelial system and non-functionalized hydrophobic entities[14,15] lead to the urgency to generate novel alternatives. Biocompatible protein substances can overcome the above mentioned problems and potentially act as an important class of bioprobes, but their limited applications resulted from much lower cost effectiveness, molar absorptivity and photobleaching thresholds.[16,17] Again, conventional fluorescent organic nanoparticles and organic dyes containing highly conjugated fluorophores such as perylene, fluorescein and rhodamine, suffer from quenching phenomena with aggregation at high concentration, which was demonstrated as aggregation caused quenching (ACQ) effect[18,19] along with poor membrane permeability and are easy photobleaching emission.[20] ACQ phenomenon practically inflicted researchers to use only dilute solution with a compromised low sensitivity for sensing applications, which is not suitable for practical utilization.[21] Thus generation of new fluorescent molecule, free from ACQ effect, along with high fluorescent efficacy are still in urgent quest and can solve the problems associated with traditional fluorophores by providing a new platform for developing novel sensors.

Search for efficient luminescent materials lead to explore further the concept of aggregation induced emission (AIE).[22] The compounds possessing AIE characteristics can emit intense fluorescence in the aggregated state, just opposite to ACQ effect.[23] This novel AIE phenomenon has great practical applications because it permits the use of the solution consisting fluorescence molecule with any concentration for sensing and lead to develop ‘‘turn-on’’ biosensors through advantageous luminogenic aggregation.[24,25] The higher sensitivity and better accuracy are associated with the ‘‘turn-on’’ feature of AIE biosensors than the ACQ methods. A number of AIE fluorogens in presence or absence of conventional fluorophore, such as siloles, cyano-substituted diarylethelene, tetraphenylethene, triphenylethene, distyrylanthracene derivatives and other architectures have been designed, synthesized and extensively studied for potential sensing and biological applications.[18]

Presently, various small or low molecular weight molecules with AIE features attracted a great attention due to several advantages like high sensitivity and selectivity with different target molecules, easy synthesis and storage, low cost, low toxicity, excellent stability toward different experimental conditions with potential biological applications;[26]

e.g cyclization induced fluorogenic response from nonfluorophoric small molecule based on 2-(2-hydroxybenzylidene)-malononitrile with potential capacity to detect nerve agents, which regulate the central nervous system by stalling the nerve impulse, are reported in literature.[27] Specific functional properties was associated by different substituents of AIEgens.[20] To widen the approach, in this work we demonstrated unexpected fluorescence behavior in water originating from a novel conventional fluorophore free zwitterionic side chain bearing *N*-substituted maleimide based small molecular unit through aggregation, which may add a new dimension to biosensing application.[28] The emission response could be easily detected by naked eye.

2. MATERIALS AND METHODS

2.1. Materials. Furan (98 %) was obtained from Spectrochem, India. Maleic anhydride (99%) was received from Lobachemie, India.1,3-Propane sultone, 2-(dimethylamino)ethyl methacrylate (DMAEMA) were purchased from Sigma-Aldrich. Triethylamine (TEA, 99%), sodium chloride (NaCl), tetrahydrofuran (THF), toluene, diethylether, isopropyl alcohol and methanol (MeOH) were obtained from Merck, India. *N*,*N*-Dimethylethylenediamine, HPLC water were received from Sisco Research Laboratories Pvt. Ltd. (SRL), India. $CDCl_3$ (99.8% D) and D_2O (99% D) were purchased from Cambridge Isotope Laboratories, Inc., USA for NMR study. The solvents such as hexanes (mixture of isomers), ethyl acetate (EA), acetone etc. were purified by standard procedures.

2.2. Instrumentation. NMR spectra were acquired in a Bruker Avance^{III} 500 MHz spectrometer at 25 ^{o}C. Positive mode electrospray ionization mass spectrometry (ESI-MS) was carried out on a Q-Tof Micro YA263 high resolution (Waters Corporation) mass spectrometer in HPLC grade water. UV-Vis spectroscopic study was monitored by a Perkin-Elmer Lambda 35 spectrophotometer. Fluorescence emission and excitation spectra were recorded on a Horiba Jobin Yvon (Fluoromax-3, Xe-150 W, 250−900 nm) fluorescence spectrometer.

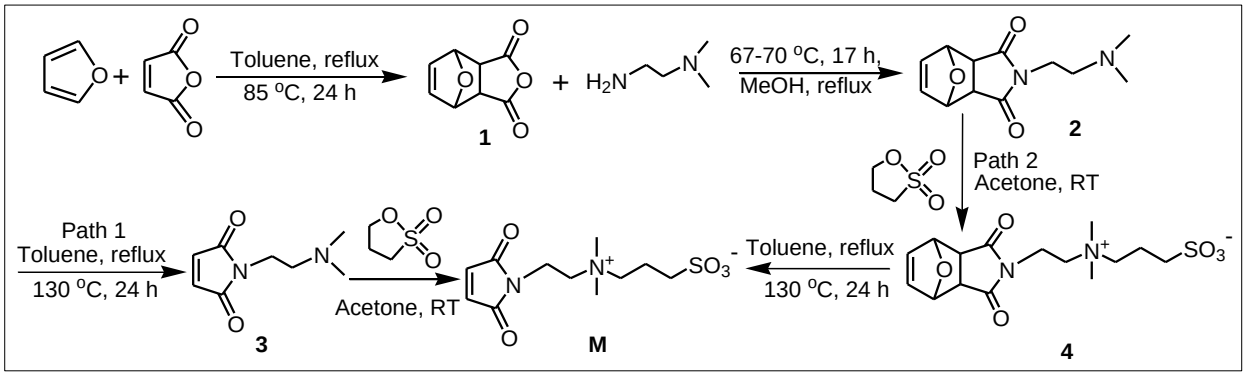

Scheme 1. Synthetic scheme for the preparation of *N*-(ethyl sulfobetaine) maleimide (M).

2.3. Synthesis of *N*-(Ethyl Sulfobetaine) Maleimide (M) *via* Path 1. The molecule (**M**) was designed to bear maleimide and zwitterionic moiety. Hence, the desired molecule, **M** was synthesized in two different pathways (path 1 and 2) as presented in Scheme 1. Path 1 involved the production of intermediate compounds: **1**, **2** and **3** to generate **M**.

(a) Synthesis of Compound (1). Furan (6.9 g, 101.9 mmol) and maleic anhydride (10.0 g, 101.9 mmol) were dissolved in 150 mL toluene in a 250 mL round bottom flask and the mixture was refluxed at 85 °C for 24 h. Then the solution was cooled down to room temperature. White crystals were obtained after cooling which were washed with diethyl ether (4 × 30 mL). After drying, compound **1** was obtained as white crystals with a yield of 60%. ^{1}H NMR ($CDCl_3$, δ, ppm, Figure S1): 6.55 (t, 2H, C***H***=C***H***), 5.44 (t, 2H, C***H***-O-C***H***), 3.15 (s, 2H, C***H***-C***H***).

(b) Synthesis of Compound (2). Compound **1** (5.0 g, 30.0 mmol) was dissolved in 100 mL methanol and placed in an ice-water bath under N_2 purging condition for 20 min. *N*,*N*-Dimethylethylenediamine (2.7 g, 30.0 mmol) and triethylamine (3.0 g, 30.0 mmol) were added dropwise under N_2 atmosphere. The reaction mixture was then refluxed at 67 °C for 14 h after which 10 % *N*,*N*-dimethylethylenediamine was further added to the mixture and the temperature was increased to 70 °C. After 2 h, the mixture was cooled to room temperature and white crystals were precipitated. They were washed with isopropyl alcohol and dried to obtain compound **2** with 50 % yield. ^{1}H NMR ($CDCl_3$, δ, ppm, Figure S2): 6.47 (t, 2H, C***H***=C***H***), 5.22 (t, 2H, C***H***-O-C***H***), 3.56 (t, 2H, NC***H₂***$CH_2N(CH_3)_2$), 2.83 (s, 2H, C***H***-C***H***), 2.45 (t, 2H, NCH_2C***H₂***$N(CH_3)_2$), 2.22 (s, 6H, $CH_2N(C$***H₃***$)_2$).

(c) Synthesis of Compound (3). Compound **3** was synthesized *via* retro-Diels-Alder reaction. 3.0 g of compound **2** was dissolved in 100 mL toluene in a 250 mL round bottom flask containing

a magnetic stir bar and the mixture was refluxed at 130 °C for 24 h. After evaporating the solvent, the crude product was purified through liquid chromatography using EA/hexanes (1:1, v/v) mixture as eluent. The product was obtained as white solid with 50% yield. ^{1}H NMR ($CDCl_3$, δ, ppm, Figure S3): 6.65 (t, 2H, C***H***=C***H***), 3.60 (t, 2H, NC***H₂***$CH_2N(CH_3)_2$), 2.46 (t, 2H, NCH_2C***H₂***$N(CH_3)_2$), 2.20 (s, 6H, $CH_2N(C$***H₃***$)_2$).

(d) Synthesis of *N*-(Ethyl Sulfobetaine Maleimide) (M). Compound **3** (3.0 g, 17.8 mmol) was dissolved in 20 mL acetone in a 100 mL round-bottomed flask and allowed to stir for 30 min. Then, 1,3-propane sultone (2.2 g, 17.8 mmol) was added at room temperature under nitrogen atmosphere. The reaction mixture was kept for 12 h under stirring condition. The solution was filtered and the white solid precipitate was washed with cold acetone for three times. The solid was dried under vacuum and the product was obtained as yellowish white solid with 70 % yield. Pure compound (**M**) was characterized by ^{1}H NMR spectroscopy (integration values are given in inset). ^{1}H NMR (D_2O, δ, ppm, Figure 1): 6.80 (t, 2H, C***H***=C***H***), 4.05 (t, 2H, NC***H₂***$CH_2N^+(CH_3)_2$-), 3.55 (m, 4H, NCH_2C***H₂***$N^+(CH_3)_2$-, N-CH_2CH_2C***H₂***SO_3^-), 3.22 (s, 6H, $NCH_2CH_2N^+(C$***H₃***$)_2$-), 3.00 (t, 2H, N-C***H₂***$CH_2CH_2SO_3^-$), 2.30 (m, 2H, N-CH_2C***H₂***$CH_2SO_3^-$).

2.4. Synthesis of *N*-(Ethyl Sulfobetaine Maleimide) (M) *via* Path 2.

(a) Synthesis of Compound (4). Compound **2** (3.0 g, 12.7 mmol) was dissolved in 20 mL acetone in a 100 mL round-bottomed flask and allowed to stir for 30 min. Then, 1,3-propane sultone (1.5 g, 12.7 mmol) was added at room temperature under nitrogen atmosphere. The reaction mixture was kept for 12 h under stirring condition. The solution was filtered and the white solid precipitate was washed with cold acetone for three times. The solid product (compound **4**) was dried under vacuum and obtained as yellowish white solid with 40 % yield and was characterized by ^{1}H NMR spectroscopy. ^{1}H NMR (D_2O, δ, ppm, Figure S4): 6.50 (t, 2H, C***H***=C***H***), 5.22 (t, 2H, C***H***-O-C***H***), 3.90 (t, 2H, NC***H₂***$CH_2N^+(CH_3)_2$-), 3.50 (m, 4H, NCH_2C***H₂***$N^+(CH_3)_2$-, N-CH_2CH_2C***H₂***SO_3^-), 3.05 (s, 6H, $NCH_2CH_2N^+(C$***H₃***$)_2$-), 2.84 (m, 4H, C***H***-C***H***, N-C***H₂***$CH_2CH_2SO_3^-$), 2.09 (m, 2H, N-CH_2C***H₂***$CH_2SO_3^-$).

(b) Synthesis of *N*-(Ethyl Sulfobetaine) Maleimide (M). Final compound, **M** was synthesized *via* retro-Diels-Alder reaction. 2.0 g of compound **4** was dissolved in 100 mL toluene in a 250 mL round bottom flask containing a magnetic stir bar and the mixture was refluxed to 130 °C for 24 h. After evaporating the solvent, the crude product was purified through washing with

methanol, acetone and diethylether. The mother compound **4** was almost gone through washing. The product was obtained as yellowish white solid with 65% yield and was characterized by ^{1}H NMR study. ^{1}H NMR (D_2O, δ, ppm, Figure S5): 6.80 (t, 2H, C***H***=C***H***), 3.90 (t, 2H, NC***H₂***$CH_2N^+(CH_3)_2$-), 3.45 (m, 4H, NCH_2C***H₂***$N^+(CH_3)_2$-, N-CH_2CH_2C***H₂***SO_3^-), 3.06 (s, 6H, $NCH_2CH_2N^+(C$***H₃***$)_2$-), 2.84 (t, 2H, N-C***H₂***$CH_2CH_2SO_3^-$), 2.09 (m, 2H, N-CH_2C***H₂***$CH_2SO_3^-$). The product formation was also confirmed by ESI-MS spectrometry (Figure S6)

(c) Synthesis of Sulfobetaine Methacrylate (SBMA). DMAEMA (3.0 g, 19.0 mmol) was dissolved in 20 mL acetone in a 100 mL round-bottomed flask and allowed to stir for 30 min. Then, 1,3-propane sultone (2.3 g, 19.0 mmol) was added at room temperature under nitrogen atmosphere. The reaction mixture was kept for 12 h under stirring condition. The solution was filtered and the white solid precipitate was washed with cold acetone for three times. The solid was dried under vacuum and dissolved in methanol. Then the solution was added to a large volume of diethyl ether and kept in refrigerator overnight to get purified product. The last step was repeated two times and pure monomer was characterized by ^{1}H NMR spectroscopy (Figure S7).

2.5. Computational Details. We perform Density Functional Theory (DFT) calculations by using Gaussian 09 package.[29] All the calculations are performed through dispersion corrected unrestricted Becke's three parameter hybrid exchange functional[30] combined with Lee-Yang-Parr non-local correlation function,[31] abbreviated as B3LYP. We have used 6-311G (d, p) basis set in all cases with the conductor-like polarizable continuum model (PCM) for the solvent as implemented in Gaussian 09. In this study we have used water as the solvent. All the structures are optimized to their minimum energy states without any symmetry constraint and confirmed by the harmonic vibrational frequency having no imaginary node. The convergence thresholds for energy optimization are set to 0.000015 Hartree/Bohr for the forces, 0.00006 Å for the displacement and 106 Hartree for the energy change.

3. RESULTS AND DISCUSSION

As mentioned in Scheme 1, each of the intermediates and **M** were characterized by ^{1}H NMR (Figure S1-S3 and 1). Integration of each peak for desired **M** matches well and no

impurity was left as shown in Figure 1. Path 2 proceeded through a new intermediate compound **4**, generated from compound **2**, which ultimately ended up to our desired molecule **M** (Scheme 1). Compound **4** and **M** formed by path 2 were characterized by ^{1}H NMR spectroscopy (Figure S4 and S5). The logic behind choosing two different pathways lied to compare the yield and the extent of purification of **M**. Conversion of **M** from intermediate compound **4** could not involve column purification due to attachment of charged group at **4**, only precipitation method was applied which resulted greater loss of product and lower yield. Also, some extent of compound **4** was left as shown in ^{1}H NMR spectrum. Hence, path 1 facilitated over path 2 in terms of compound purity as well as yield. Hence, we further preceded all our spectroscopic analysis with most pure **M** obtained by path 1. The desired molecule, **M** formation was further confirmed by electrospray ionization mass spectrometry (ESI-MS) (Figure S6) with [**M** + H]$^{+}$ = 291.45 *m*/*z*, which matches nicely with the calculated [**M** + H]$^{+}$ = 291.09 *m*/*z*.

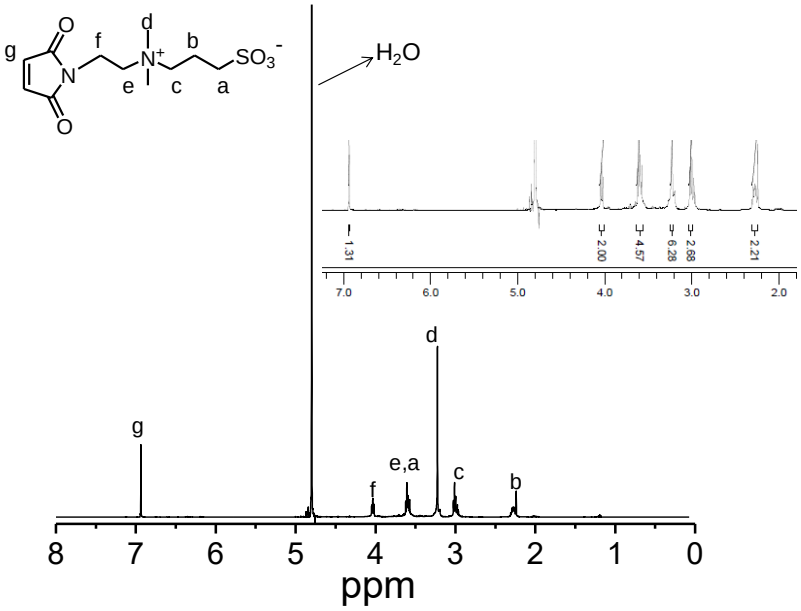

Figure 1. ^{1}H NMR spectrum of **M** in D_2O with integration values (*via* path 1).

The molecule **M** was readily water soluble at room temperature due to presence of zwitterionic group.[32] Concentration dependent UV-visible absorbance spectra of **M** were represented by Figure S8. Initially the absorption spectrum of **M** in water with concentration 4.50 mM was characterized by the peak at 290 nm. The effect of

concentration on absorbance value demonstrated by measuring UV-visible absorbance spectra by dilution of 4.50 mM solution to 2.25, 0.90, 0.45, 0.22, 0.15 mM. An additional peak at 217 nm was appeared on dilution. Decreasing the concentration of the solution from 4.50 mM to 0.15 mM resulted a gradual drop of absorption intensity of those peaks because of dilution effect according to Lambert Beer Law.[33] The peak at 290 nm almost disappeared for 0.15 mM solution.

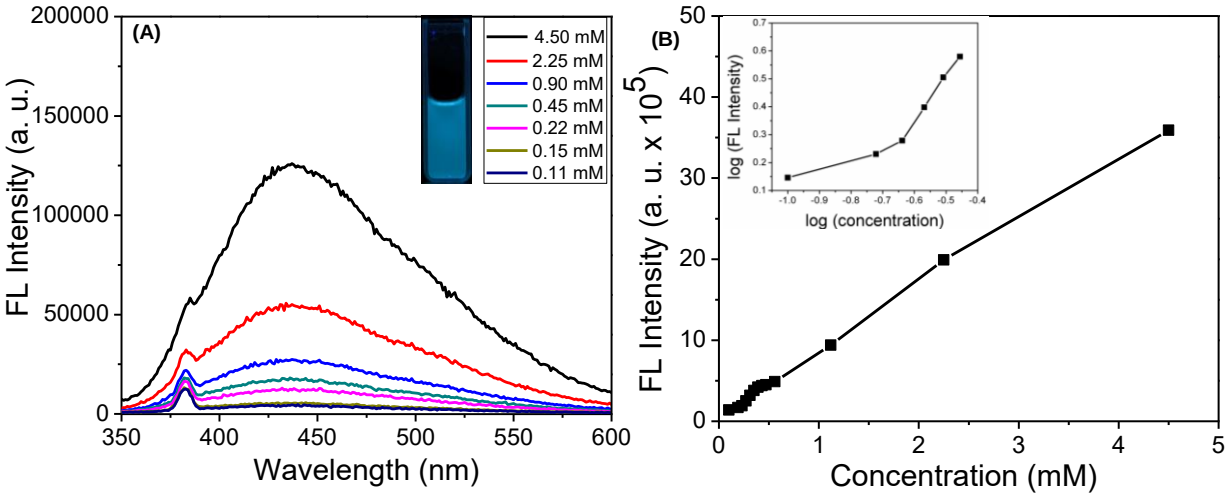

Figure 2. (A) Concentration dependent fluorescence spectra of **M** in water (all the data at low concentration are not shown due to lack of clarity). The inset shows fluorescence images of **M** solutions upon excitation with UV light at 366 nm, (B) linear plot of fluorescence dependency with concentration (inset shows the log plot).

Despite absence of any classical fluorescent probe, the aqueous solution of **M** demonstrated a considerable photoluminescence even at lower threshold concentration (~0.20 mM) under UV irradiation (Figure 2 and S9A). The higher concentrations were also chosen to study (2.25, 4.50 mM) which are high enough in terms of biological applications, only because at those concentrations the UV peak at 290 nm is most prominent. **M** exhibited characteristics UV absorption at 217, 290 nm. Additionally, a non-negligible absorbance between the range of 300-350 nm was observed (molar extension coefficient, $\varepsilon = 17 \times 10^{-2}$ L mol^{-1} cm^{-1} at 300 nm; 17×10^{-3} L mol^{-1} cm^{-1} at 350 nm). The molecule emits in blue region only upon excitation above 300 nm. Best emission was observed upon excitation range from 330 to 400 nm (Figure S10). Comparative fluorescence emission spectra of M

with several intermediate compounds produced *via* path 1 and 2 choosing variable excitation wavelength (330, 400 and 450 nm) revealed in Figure S9B and S10. The emission intensity of compounds **1** and **2** was recorded in tetrahydrofuran (THF) and much lower emission was observed compared to aqueous solution of **M** specifically at lower concentration (Figure S9B), hence demonstrating nonfluorescent intermediates. The explanation might be as follows. Introduction of hydrophilic moieties such as quaternary ammonium, phosphate as well as sulfonate units to the AIEgens can donate high water solubility, again intensified emission resulting from electrostatic interaction between cationic and anionic functionality are already reported.[34] For example, cationic silole molecule was nonemissive in aqueous solution, but its emission was intensified in the presence of DNA because of the formation and aggregation of silole–DNA complex.[35] Hence, the presence of zwitterionic part containing a quaternary ammonium and sulfonate attached to **M** might play major role to emission enhancement compared to the intermediates through a particular alignment in solution phase *via* electrostatic interaction.

Another comparison with nonfluorescent zwitterionic sulfobetainemethacrylate (SBMA) (characterized by ^{1}H NMR spectroscopy as represented in Figure S7) solution (4.50 mM) was made (Figure S11) to demonstrate that, only zwitterionic part or double bond was not solely responsible to show unexpected fluorescence, but proper orientation of **M** in solution through aggregation might be the possible reason. The effect of concentration of aqueous solution containing **M** was highly pronounced as demonstrated in Figure 2A with an excitation at 330 nm. The emission intensity almost disappeared at very low concentration (0.11 mM). This phenomenon was another indirect evidence of small molecular aggregation in aqueous solution to induce unexpected fluorescence emission, which diminished upon dilution due to lack of driving force responsible for molecular gathering below a certain concentration level. The inset of Figure 2B shows the concentration dependency of FL intensity especially at lower concentration range. The plot shows that insensitivity of the FL emission up to 0.30 mM, is nearly insensitive to the concentration of the *N*-substituted maleimide molecules whereas sudden increase in FL emission intensity was observed at the concentration of 0.30 mM and above this concentration the emission intensity increases with the concentration. This indicates that the enhancement of emission intensity may be due to aggregation of *N*-substituted

maleimide molecules in solution, which was further verified by theoretical analysis (*vide infra*).

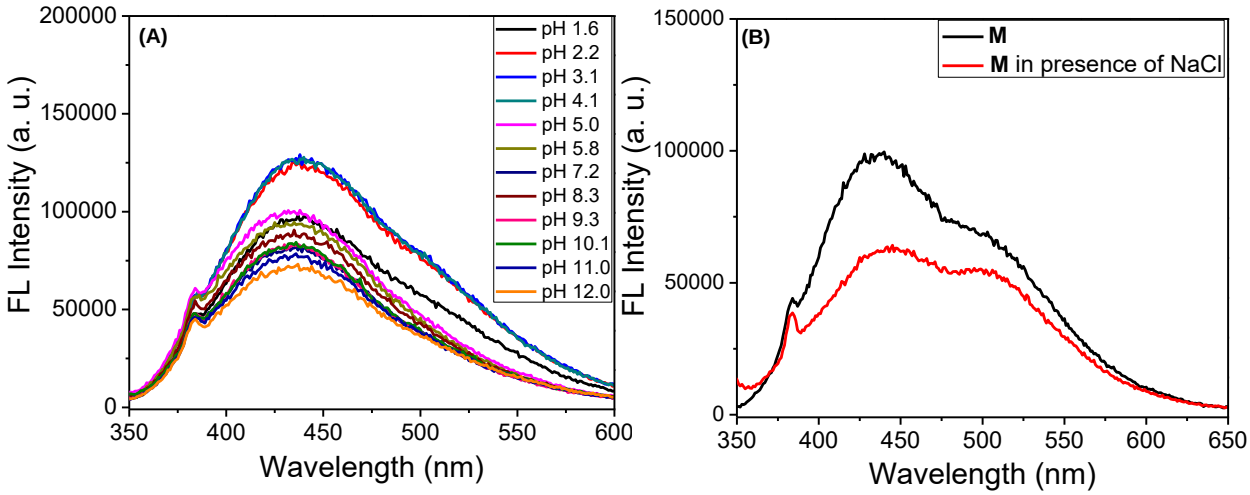

Figure 3. (A) pH dependent fluorescence spectra of **M** in water, with concentration 4.50 mM, (B) fluorescence emission spectra of **M** in presence of saturated NaCl solution (6.80 M).

The photoluminescence efficacy of **M** at 4.50 mM concentration with a constant excitation at 330 nm was also determined by changing the solution pH (Figure 3A), as pH is another important factor to dictate biomedical sensing applicability.[36] AIE under selective pH range can be suitable in some biomolecular sensing like proteins or DNA or drug release.[37] Herein, pH could not directly affect to diminish the emission efficacy completely unlike to the concentration factor. However, some selectivity in acidic pH was observed. A gradual decrease in emission was resulted with increasing pH 1.6 to 12.0 with highest efficiency in pH range 2.0 to 4.0. Figure 3B revealed the salting out effect of photoluminescence efficiency of 4.50 mM solution of **M** in water with excitation wavelength 330 nm. The decrease in emission intensity by addition of a saturated solution of sodium chloride (NaCl) (6.80 M) was resulted from the interaction of zwitterionic part attached to **M** with Na^+ and Cl^- ions. That phenomenon demonstrated the role of zwitterionic functionality in small molecular aggregation which induced the emission.

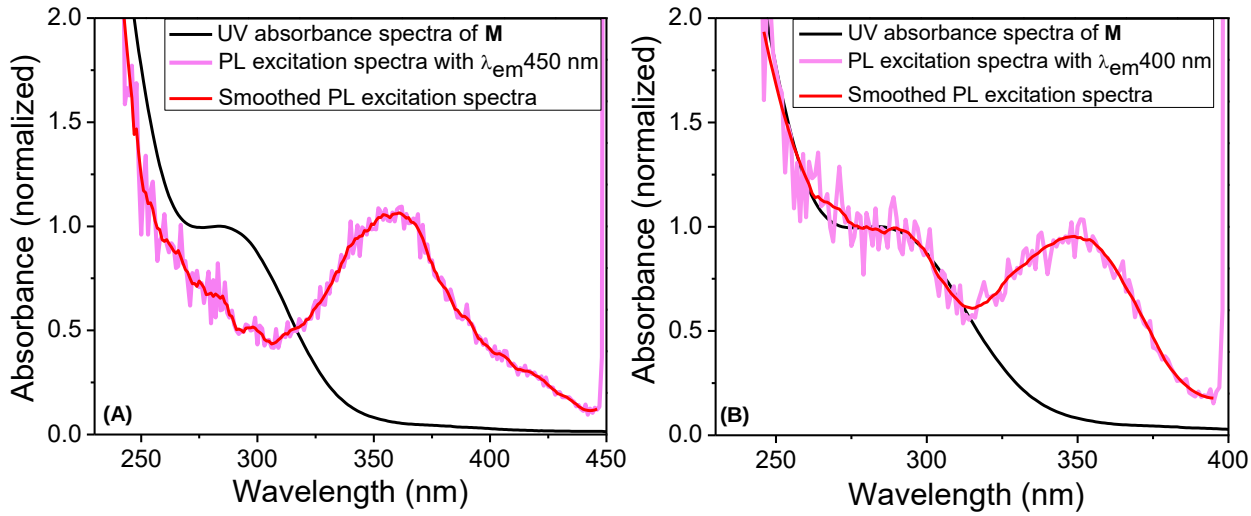

Figure 4. Normalized PL excitation spectra of **M** in water in comparison with UV absorbance at emission wavelength (λ_{em}) (A) 450 nm, (B) 400 nm.

Figure 4A presents the normalized photoluminescence (PL) excitation spectra of 4.50 mM solution of **M** in water with maximum emission wavelength 450 nm in comparison to UV absorbance value. The spectra expressed a dominant excitation peak at 360 nm, responsible for the broad fluorescence emission maxima. Interestingly, that particular peak is absent in optical absorbance spectra. Further, PL excitation spectra was also recorded with disparity of emission wavelengths 400 (Figure 4B) and 550 nm (Figure S12) and the new excitation peak was generated at the same position, nearly 360 nm. The peak at 290 nm, as observed in ground state optical absorbance spectra, was also generated in PL excitation spectra up to 400 nm emission wavelength (Figure 4B), which regulated the emission of **M** below visible range. This phenomenon reflected the presence of single aggregated species generated from proper orientation in solution with an excitation wavelength 360 nm, which is solely responsible for this broad range unexpected fluorescence in visible wavelength.

We have computed UV-visible spectra by using time dependent density functional theory (TDDFT)[38] to gain microscopic understanding about the appearance of excitation peak with an excitation wavelength 360 nm. In all cases, excitation energies and oscillator strengths are computed for ten lowest singlet excited states by single canonical excitation. For UV-visible spectra, we use ground state optimized geometry in the TDDFT method with same functional and basis set used in their geometry optimization. Hence, excitation

energies used to compute the UV-visible spectra is adiabatic excitation. We have used up to six **M** molecules to determine optimized structures of different aggregated structures. In the density functional theory study, we have computed UV-visible spectra of a single **M** molecules (monomer) as well as aggregation of 2 (dimer), 3 (trimer), 4 (tetramer) and 6 (hexamer) **M** molecules. The optimized structures of the monomer and their aggregations are shown in the supporting information (Figure S13-S17). The aggregation occurs mainly due to strong electrostatic interaction between negative charge on the sulfonate [$–SO_3^-$] group and positive on the nitrogen atom of the alkyl chain.

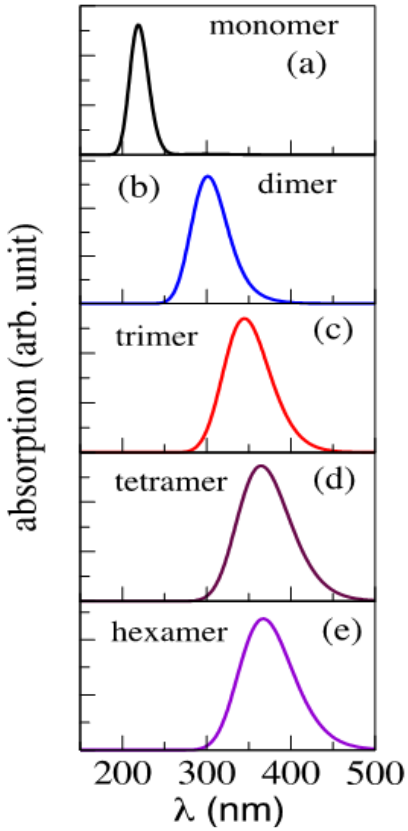

Figure 5. UV-visible spectra computed through TDDFT for (a) single M molecule (monomer), aggregation of (b) 2 (dimer), (c) 3 (trimer), (d) 4 (tetramer) and (e) 6 (hexamer) M molecules.

The UV-visible spectra obtained from the optimized structure of the monomer and their aggregations for different number of monomers are shown in Figure 5. The absorption maxima of **M** in water for a monomer is observed at 217 nm (Figure 5a), matches very well

with the experimental UV-spectra at very dilute solution that is at 0.15 mM concentration (Figure S8). For the dimer, the peak in UV-spectra was observed at 301 nm. The red-shift of the absorption peak by 84 nm is due to the aggregation of two M molecules. The shortest distance between two **M** molecules in the dimer is ~3.67 Å which is the distance between $[NMe_2R_2]^+$ and $[SO_3]^-$. This suggests that non-bonded electrostatic interaction plays a major role in the aggregation process. Further, the absorption peak for the trimer was observed at 344 nm (Figure 5c) indicating red shift of the peak by 43 nm. For the aggregation of four monomers (tetramer), a peak at 362 nm was appeared with a red shift of the peak by 18 nm. The wavelength of the absorption peak matches excellently with the experiment. For hexamer also, we observed the peak of UV-spectra at 362 nm indicating no shift of the absorption due to further aggregation. These confirmed that aggregation of **M** in aqueous solution is solely responsible for this broad range unexpected fluorescence observed experimentally in the visible wavelength.

4. CONCLUSIONS

In summary, a completely new and traditional fluorophore free water soluble maleimide functionalized with zwitterionic side chain, **M**, was successfully synthesized with its potential AIE properties. PL spectra suggested that an excitation wavelength 360 nm is solely responsible for the broad range unexpected fluorescence in visible wavelength. The particular orientation of the zwitterionic functionality in solution resulted the aggregation which further confirmed by theoretical TDDFT calculations. This study exhibited a maximum UV-spectrum at 362 nm up to tetrameric aggregation, after that a saturation was achieved. The blue light emitting characteristics of **M** opened a new dimension to modern biosensing applications.[39]

ASSOCIATED CONTENT

Supporting Information

The Supporting Information is available herewith.

AUTHOR INFORMATION

Corresponding Authors * E-mail: ishitamukherjee08@gmail.com

ACKNOWLEDGMENTS

I thank the Science and Engineering Research Board (SERB), Council of Scientific and Industrial Research (CSIR) and Government of India for my fellowship and research grands during my Ph.D in Indian Institute of Science Education and Research, Kolkata and Postdoctoral journey in the University of Burdwan. I acknowledge **Prof. Bimalendu Ray** (Chemistry department, The University of Burdwan), **Prof. Priyadarsi De**, (Polymer Research Centre, Department of Chemical Sciences, Indian Institute of Science Education and Research Kolkata**), Prof. Debansu Chaudhuri** (Department of Chemical Sciences, Indian Institute of Science Education and Research Kolkata) for many helpful discussions and laboratory use. I thank **Prof Pradip Kr. Ghorai** (Department of Chemical Sciences, Indian Institute of Science Education and Research Kolkata) for helping me in theoretical calculation.

5. REFERENCES

(1) Sagara, Y.; Yamane, S.; Mitani, M.; Weder, C.; Kato, T. Mechanoresponsive Luminescent Molecular Assemblies: An Emerging Class of Materials. *Adv. Mater.* **2016**, *28*, 1073-1095.

(2) Yao, J.; Yang, M.; Duan, Y. Chemistry, Biology, and Medicine of Fluorescent Nanomaterials and Related Systems: New Insights into Biosensing, Bioimaging, Genomics, Diagnostics, and Therapy. *Chem. Rev.* **2014**, *114*, 6130-6178.

(3) Sun, G.; Berezin, M. Y.; Fan, J.; Lee, H.; Ma, J.; Zhang, K.; Wooley, K. L.; Achilefu, S. Bright Fluorescent Nanoparticles for Developing Potential Optical Imaging Contrast Agents. *Nanoscale* **2010**, *2*, 548-558.

(4) Zhou, Y.; Yoon, J. Recent Progress in Fluorescent and Colorimetric Chemosensors for Detection of Amino Acids. *Chem. Soc. Rev.* **2012**, *41*, 52-67.

(5) Zhou, Y.; Xu, Z.; Yoon, J. Fluorescent and Colorimetric Chemosensors for Detection of Nucleotides, FAD and NADH: Highlighted Research During 2004-2010. *Chem. Soc. Rev.* **2011**, *40*, 2222-2235.

(6) Disney, M. D.; Zheng, J.; Swager, T. M.; Seeberger, P. H. Detection of Bacteria with Carbohydrate-Functionalized Fluorescent Polymers. *J. Am. Chem. Soc.* **2004**, *126*, 13343-13346.

(7) Jia, X.; Zhao, X.; Tian, K.; Zhou, T.; Li, J.; Zhang, R.; Liu, P. Fluorescent Copolymer-Based Prodrug for pH-Triggered Intracellular Release of DOX. *Biomacromolecules* **2015**, *16*, 3624-3631.

(8) Doré, K.; Dubus, S.; Ho, H.-A.; Lévesque, I.; Brunette, M.; Corbeil, G.; Boissinot, M.; Boivin, G.; Bergeron, M. G.; Boudreau, D.; Leclerc, M. Fluorescent Polymeric Transducer for the Rapid, Simple, and Specific Detection of Nucleic Acids at the Zeptomole Level. *J. Am. Chem. Soc.* **2004**, *126*, 4240-4244.

(9) Feng, X.; Liu, L.; Wang, S.; Zhu, D. Water-Soluble Fluorescent Conjugated Polymers and Their Interactions with Biomacromolecules for Sensitive Biosensors. *Chem. Soc. Rev.* **2010**, *39*, 2411-2419.

(10) Zhang, X.; Wang, S.; Liu, M.; Yang, B.; Feng, L.; Ji, Y.; Tao, L.; Wei, Y. Size Tunable Fluorescent Nano-Graphite Oxides: Preparation and Cell Imaging Applications. *Phys. Chem. Chem. Phys.* **2013**, *15*, 19013-19018.

(11) Hui, J.; Zhang, X.; Zhang, Z.; Wang, S.; Tao, L.; Wei, Y.; Wang, X. Fluoridated HAp:Ln3+ (Ln = Eu or Tb) Nanoparticles for Cell-Imaging. *Nanoscale* **2012**, *4*, 6967-6970.

(12) Zhang, X.; Wang, S.; Zhu, C.; Liu, M.; Ji, Y.; Feng, L., Tao, L.; Wei, Y. Carbon-Dots Derived from Nanodiamond: Photoluminescence Tunable Nanoparticles for Cell Imaging. *J. Colloid Interface Sci.* **2013**, *397*, 39–44.

(13) Lee, D.-E.; Koo, H.; Sun, I.-C.; Ryu, J. H.; Kim, K.; Kwon, I. C. Multifunctional Nanoparticles for Multimodal Imaging and Theragnosis. *Chem. Soc. Rev.* **2012**, *41*, 2656-2672.

(14) Chandra, S.; Das, P.; Bag, S.; Laha, D.; Pramanik, P. Synthesis, Functionalization and Bioimaging Applications of Highly Fluorescent Carbon Nanoparticles. *Nanoscale* **2011**, *3*, 1533-1540.

(15) Wu, X.; He, X.; Wang, K.; Xie, C.; Zhou, B.; Qing, Z. Ultrasmall Near-Infrared Gold Nanoclusters for Tumor Fluorescence Imaging In Vivo. *Nanoscale* **2010**, *2*, 2244-2249.

(16) Day, R. N.; Davidson, M. W. The Fluorescent Protein Palette: Tools for Cellular Imaging. *Chem. Soc. Rev.* **2009**, *38*, 2887-2921.

(17) Cai, Z.; Ye, Z.; Yang, X.; Chang, Y.; Wang, H.; Liu, Y.; Cao, A. Encapsulated Enhanced Green Fluorescence Protein in Silica Nanoparticle for Cellular Imaging. *Nanoscale* **2011**, *3*, 1974-1976.

(18) Bromfield, S. M.; Wilde, E.; Smith, D. K. Heparin Sensing and Binding-Taking Supramolecular Chemistry Towards Clinical Applications. *Chem. Soc. Rev.***2013**, *42*, 9184-9195.
(19) Yuan, W. Z.; Lu, P.; Chen, S.; Lam, J. W. Y.; Wang, Z.; Liu, Y.; Kwok, H. S.; Ma, Y.; Tang, B. Z. Changing the Behavior of Chromophores from Aggregation-Caused Quenching to Aggregation-Induced Emission: Development of Highly Efficient Light Emitters in the Solid State. *Adv. Mater.* **2010**, *22*, 2159-2163.
(20) Zhang, X.; Zhang, X.; Tao, L.; Chi, Z.; Xu, J.; Wei, Y., Aggregation Induced Emission-Based Fluorescent Nanoparticles: Fabrication Methodologies and Biomedical Applications. *J. Mater. Chem. B* **2014**, *2*, 4398-4414.
(21) Kwok, R. T. K.; Leung, C. W. T.; Lam, J. W. Y.; Tang, B. Z. Biosensing by Luminogens with Aggregation-Induced Emission Characteristics. *Chem. Soc. Rev.* **2015**, *44*, 4228-4238.
(22) Mei, J.; Hong, Y.; Lam, J. W. Y.; Qin, A.; Tang, Y.; Tang, B. Z. Aggregation-Induced Emission: The Whole Is More Brilliant than the Parts. *Adv. Mater.* **2014**, *26*, 5429-5479.
(23) Mei, J.; Leung, N. L. C.; Kwok, R. T. K.; Lam, J. W. Y.; Tang, B. Z. Aggregation-Induced Emission: Together We Shine, United We Soar! *Chem. Rev.* **2015**, *115*, 11718-11940.
(24) Saha, B.; Bauri, K.; Bag, A.; Ghorai, P. K.; De, P. *Polym. Chem.* **2016**, *7*, 6895-6900.
(25) Bauri, K.; Saha, B.; Mahanti, J.; De, P. *Polym. Chem.* **2017**, *8*, 7180-7187.
(26) Zhang, X.; Yin, J.; Yoon, J. Recent Advances in Development of Chiral Fluorescent and Colorimetric Sensors. *Chem. Rev.* **2014**, *114*, 4918-4959.
(27) Ali, S. S.; Gangopadhyay, A.; Pramanik, A. K.; Samanta, S. K.; Guria, U. N.; Manna, S.; Mahapatra, A. K. Real Time Detection of the Nerve Agent Simulant Diethylchlorophosphate by Nonfluorophoric Small Molecules Generating a Cyclization-Induced Fluorogenic Response. *Analyst* **2018**, *143*, 4171-4179.
(28) Baker, B. R.; Lai, R. Y.; Wood, M. S.; Doctor, E. H.; Heeger, A. J.; Plaxco, K. W. An Electronic, Aptamer-Based Small-Molecule Sensor for the Rapid, Label-Free Detection of Cocaine in Adulterated Samples and Biological Fluids. *J. Am. Chem. Soc.*, **2006**, *128*, 3138–3139.
(29) Gaussian 09, Revision D.01, Frisch, M. J.; Trucks, G. W.; Schlegel, B. H.; Scuseria, G. E.; Robb, M. A.; Cheeseman, J. R.; Scalmani, G.; Barone, V.; Mennucci, B.; Petersson, G. A.; Nakatsuji, H.; Caricato, M.; Li, X.; Hratchian, P. H.; Izmaylov, A. F.; Bloino, J.; Zheng, G.; Sonnenberg, J. L.; Hada, M.; Ehara, M.; Toyota, K.; Fukuda, R.; Hasegawa, J.; Ishida, M.; Nakajima, T.; Honda, Y.; Kitao, O.; Nakai, H.; Vreven, T.; Montgomery, J. A.; Peralta, J. E. Jr.;

Ogliaro, F.; Bearpark, M.; Heyd, J. J.; Brothers, E.; Kudin, K. N.; Staroverov, V. N.; Kobayashi, R.; Normand, J.; Raghavachari, K.; Rendell, A.; Burant, J. C.; Iyengar, S. S.; Tomasi, J.; Cossi, M.; Rega, N.; Millam, J. M.; Klene, M.; Knox, J. E.; Cross, J. B.; Bakken, V.; Adamo, C.; Jaramillo, J.; Gomperts, R.; Stratmann, R. E.; Yazyev, O.; Austin, A. J.; Cammi, R.; Pomelli, C.; Ochterski, J. W.; Martin, R. L.; Morokuma, K.; Zakrzewski, V. G.; Voth, G. A.; Salvador, P.; Dannenberg, J. J.; Dapprich, S.; Daniels, A. D.; Farkas, O.; Foresman, J. B.; Ortiz, J. V.; Cioslowski, J.; Fox, D. J. Gaussian, Inc. Wallingford CT, 2009.

(30) Becke, A. D. Density-Functional Exchange-Energy Approximation with Correct Asymptotic Behavior. *Phys. Rev. A* **1988**, *3*8, 3098–3100.

(31) Lee, C.; Yang, W.; Parr, R. G. Development of the Colle-Salvetti Correlation-Energy Formula into a Functional of the Electron Density. *Phys. Rev. B* **1988**, *37*, 785–789.

(32) Mukherjee, I.; Ghosh, A.; Bhadury, P.; De, P. Matrix Assisted Regulation of Antimicrobial Properties: Mechanistic Elucidation with Ciprofloxacin-Based Polymeric Hydrogel Against Vibrio sp. *Bioconjugate Chem.*, **2019**, *30*, 218-230.

(33) Langhals, H.; Abbt-Braun, G.; Frimmel, F. H. Association of Humic Substances: Verification of Lambert-Beer Law. *Acta Hydrochim. Hydrobiol.* **2000**, *28*, 329-332.

(34) Caruso, F.; Lichtenfeld, H.; Donth, E.; Mohwald, H. Investigation of Electrostatic Interactions in Polyelectrolyte Multilayer Films: Binding of Anionic Fluorescent Probes to Layers Assembled onto Colloids. *Macromolecules* **1999**, *32*, 2317–2328.

(35) Wang, M.; Zhang, G.; Zhang, D.; Zhu, D.; Tang, B. Z. Fluorescent Bio/Chemosensors Based on Silole and Tetraphenylethene Luminogens with Aggregation-Induced Emission Feature. *J. Mater. Chem.* **2010**, *20*, 1858-1867.

(36) Chen, S.; Hong, Y.; Liu, Y.; Liu, J.; Leung, C. W. T.; Li, M.; Kwok, R. T. K.; Zhao, E.; Lam, J. W. Y.; Yu, Y.; Tang, B. Z. Full-Range Intracellular pH Sensing by an Aggregation-Induced Emission-Active Two-Channel Ratiometric Fluorogen. *J. Am. Chem. Soc.* **2013**, *135*, 4926-4929.

(37) Lu, H.; Xu, B.; Dong, Y.; Chen, F.; Li, Y.; Li, Z.; He, J.; Li, H.; Tian, W. Novel Fluorescent pH Sensors and a Biological Probe Based on Anthracene Derivatives with Aggregation-Induced Emission Characteristics. *Langmuir* **2010**, *26*, 6838-6844.

(38) Runge, E.; Gross, E. K. U. Density-Functional Theory for Time-Dependent Systems. *Phys. Rev. Lett.* **1984**, *52*, 997-1000.

(39) Khusbu, F. Y.; Zhou, X.; Chen, H.; Ma, C.; Wang, K. *Trends Anal. Chem.* **2018**, *109*, 1-18.

For "Table of Contents" Use Only

Unexpected Fluorescent Behavior of Maleimide Based Zwitterionic Molecule: Aggregation Induced Emission

Ishita Mukherjee*